LARGE EDDY SIMULATION OF SECONDARY FLOWS OVER LONGITUDINALLY-RIDGED WALLS

Luca Falcomer
Dipartimento di Ingegneria Civile, Universitá di Trieste
Piazzale Europa 1, 34127 Trieste, Italy
falcomer@univ.trieste.it

Vincenzo Armenio
Dipartimento di Ingegneria Civile, Universitá di Trieste
Piazzale Europa 1, 34127 Trieste, Italy
armenio@univ.trieste.it

Mauro Tassan-Toffola
Dipartimento di Ingegneria Civile, Universitá di Trieste
Piazzale Europa 1, 34127 Trieste, Italy
tassanm@libero.it

ABSTRACT

In the present paper large-eddy simulations of a turbulent channel flow with longitudinal, large-amplitude ridges are carried out. This flow exhibits large secondary flows over the ridge that need to be properly simulated in order to evaluate with enough accuracy the spanwise distribution of the primary as well as the secondary wall stress. The DNS avalaible data at a low Reynolds number as well as the data from an experimental study at a moderate Reynolds number are matched. Our LES results agree satisfactorily with the DNS data at $Re_\tau = 140$, and with the experimental data at $Re_\tau = 582$. The present investigation shows that the intensity and topology of the secondary flow is dependent on the Reynolds number of the flow. The results have also shown the presence of near-wall, small and intense re-circulations which may produce localized secondary wall stresses.

INTRODUCTION

The analysis of turbulent flow over longitudinally ridged walls is relevant in hydraulic engineering, since this geometry is prototypical of sand ridges, longitudinal stripes often observed in rivers. The presence of longitudinal ridges is associated to secondary large-scale flows and secondary wall stresses.

Most past investigations have been devoted to the understanding of the primary mechanism that leads to the formation of sand ridges. Several causes have been found to contribute to the loss of stability of a erodible bed. They may be summarize as follows:

- The presence of lateral walls causes the appearance of a corner secondary flow characterized by streamwise vorticity. This large structure is confined in the corner area and does not propagate toward the center of the channel unless the bed is erodible. In the latter case, the secondary flow may produce a local trough that enhances the streamwise vorticity and generate new secondary currents. This is an unstable mechanism that, once started, may produce dramatic variations of the bed morphology (Nezu & Nakagawa, 1984);

- Non-uniform bed roughness along the spanwise direction, may produce unbalance in the normal turbulent stresses and, hence, the appearance of secondary flows that, if strong enough, can cause the loss of stability of the bed configuration and the generation of ridges (Muller, 1979; Tominaga & Nezu, 1991)

- When the free surface is present, the linear analysis of the fluid-bed system (Colombini, 1993) has shown the system to be unstable when the Froude number of the current exceeds a critical value for a wave

length of the spanwise perturbation of the same order of the flow depth.

Whatever the primary cause for the formation of a sand ridges is, its existence is always associated to the presence of a secondary flow, since, as addressed by Colombini (1993), the appearance of a sand ridge is the result of a delicate balance between the stabilizing effect of the gravitational field and the effect of the secondary shear stress which acts in the opposite direction.

Since the intensity of the secondary current is always a small percentage of the streamwise velocity, (tipically smaller than 5%) if a general criterion for the generation of the sand ridges has to be formulated, proper turbulence models are required, able to simulate accurately the secondary currents.

Standard $k-\epsilon$ models, used in conjunction with the Reynolds averaged Navier-Stokes equations (RANS), have been proven to fail in the evaluation of secondary flows characterized by streamwise vorticity. Reynolds-stress as well as non-linear $k-\epsilon$ models may be more accurate, nevertheless their performances are strongly dependent on the proper choice of empirical constants.

Recently, Large Eddy simulation (LES) has shown to be able to overcome the drawbacks associated with the use of RANS-based methods. It has proved to supply accurate results in both equilibrium and non-equilibrium wall-bounded flows, in flows over complex geometry as well as in flows characterized by the presence of secondary currents (Liu *et al.*, 1996).

In the present paper the investigation of the turbulent flow over a channel with longitudinal ridges is carried out using LES. The scope of the present work is to supply an accurate estimation of the secondary flows that is of primary importance for the successive evaluation of the associated shear stress.

MATHEMATICAL FORMULATION

In LES, the large scale, energy carrying, structures are resolved, whereas the more isotropic, small scales, are modelled by the use of a subgrid-scale (SGS) closure. In the present work, we use the curvilinear form of the filtered, incompressible Navier-Stokes equations. A dynamic mixed SGS model is used for the closure of the turbulent stresses. The model is composed by the scale similar part of Bardina *et al.* (1980) and an eddy-viscosity one (Smagorinsky, 1963). The model is treated dynamically and the constant is localized employing the Lagrangian technique of Meneveau *et al.* (1996). The model is then recast in a contravariant form in order to be used in curvilinear coordinates.

The governing equations are solved using the finite-difference fractional-step method of Zang *et al.* (1994). The algorithm is *2nd*-order accurate both in time and in space. Central differences are used for the discretization of the space-derivatives.

The flow is driven by a constant mean pressure gradient. Periodic boundary conditions are used in the streamwise as well as in the spanwise direction, whereas no-slip conditions are applied at the solid walls. The model has been extensively validated either on orthogonal and on strongly distorted grids, always supplying accurate results. A detailed description of the model and of the validation tests is in Armenio & Piomelli (2000).

NUMERICAL RESULTS

Two main investigations have been performed in the past, that studied the flow over a large amplitude ridge, namely the experimental study of Nezu and Nakagawa (1984) (hereafter referred to as NN84), and the very recent direct numerical simulation (DNS) of Kawamura and Sumori (1999) (hereafter referred to as KS99). In spite of the fact that somewhat similar flow fields were obtained in these studies, remarkable differences appear in the distribution of the wall primary stress, and in the topology of the mean secondary flows, which, in turn, affect the secondary stress over the wall.

In the present paper we show that the differences are mainly due to the fact that the DNS is carried out at a Reynolds number as small as three time that of the experiment, indeed as reported in the following, the secondary current is quite sensitive to the Reynolds number of the flow.

Hence, we first match the DNS results of KS99 and then the experimental ones of NN84. Then we discuss the flow field modifications with the Reynolds number.

LES against DNS

A simulation has been first carried out to match the results of the DNS simulation of KS99 at $Re_\tau = 140$ based on the spanwise-averaged friction velocity.

KS99 have considered a symmetrical channel equipped with a longitudinal trapezoidal

ridge over each wall. In wall-units, it is 17.5 height, 73 wide at the bottom and 36 wide at the top. KS99 accumulated the statistics over a non-dimensional time $t_{nd} = 25000\nu/u_\tau^2$ whereas, due to the computational efforts required, we have ran our computation for a non-dimensional time as large as $t_{nd} = 7000\,\nu/u_\tau^2$ which corresponds to $tu_\tau/\delta \sim 45$. The computational domain of the DNS of KS99 is $1.25\pi\delta$ long, $0.375\pi\delta$ wide and 2δ height, with a resolution $\Delta x^+ = 12.3$, $\Delta z^+ = 4.9$, $0.19 < \Delta y^+ < 4.9$ ($48 \times 96 \times 36$ grid points). In our LES we have used the same computational domain, and a coarser resolution: $\Delta x^+ = 25$, $\Delta z^+ = 5.5$, $1 < \Delta y^+ < 10$ ($24 \times 64 \times 32$ grid points). The statistics have been accumulated in time, averaged over the streamwise direction of homogeneity over the two halves of the channel, and over half ridge. Our LES results compared with the DNS data satisfactorily. Figure 1 shows a comparison between the spanwise distribution of the friction velocity $u_\tau(z) = (\nu\partial\langle u(z)\rangle/\partial n)^{1/2}$ (with n the normal coordinate to the wall surface), obtained by KS99 and with our LES. It appears that the local friction velocity (and consequently the wall stress) is very well predicted. The spanwise distribution of the friction velocity suggests that the presence of the ridge causes the primary wall stress to decrease at the bottom-corner ($z/\delta = 0.33$), whereas a rapid increase occurs in the up-slope wall, reaching the maximum value at the top-corner. There, the friction velocity exceeds the averaged value by about 25%. According to the experimental analysis of NN84, simulations predict a large-scale

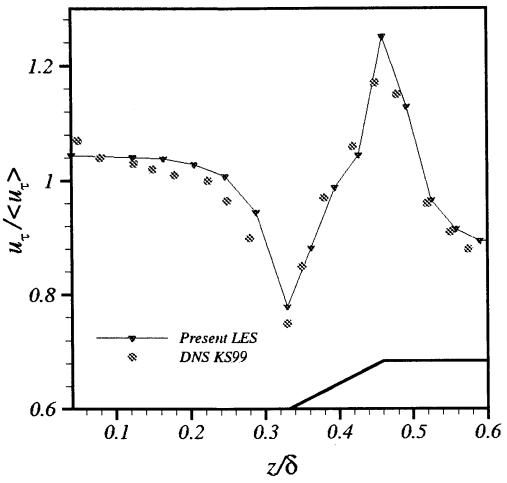

Figure 1: Spanwise distribution of the primary wall-stress evaluated with our LES and the DNS of KS99 at $Re_\tau = 140$. $< u_\tau >$ denotes the spanwise-averaged friction velocity.

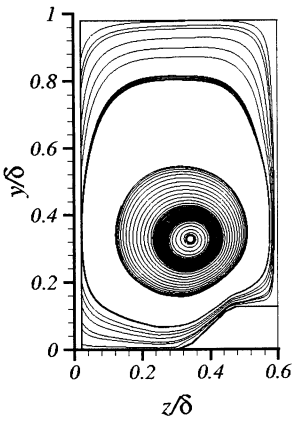

Figure 2: Contour-plot of stream-tracers of the secondary flow obtained with LES at $Re_\tau = 140$.

secondary flow (Fig. 2). The secondary flow obtained with LES is centered at $y = 0.33\delta$, $z = 0.34\delta$ (according to the frame of reference of Fig. 2), in excellent agreement with the DNS of KS99. Figure 3 shows the distribution

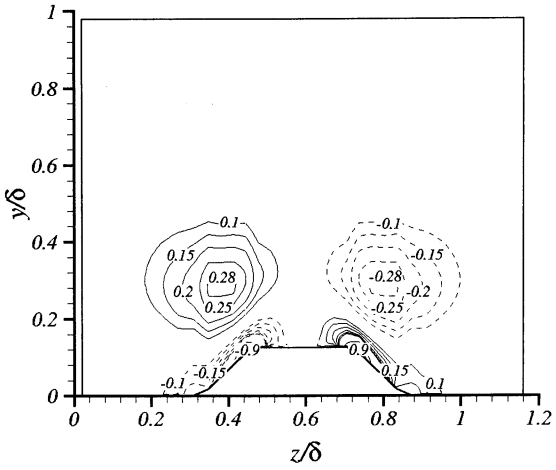

Figure 3: Contour-plot of the streamwise mean vorticity (made dimensionless with δ/U_{max}) obtained with LES at $Re_\tau = 140$.

of the mean dimensionless streamwise vorticity. It is well predicted both in magnitude and in the space-distribution by our LES computation: the maximum value reaches 0.28, against 0.32 of the DNS. The position of the peak of vorticity ($y = 0.28\delta$, $z = 0.37\delta$) doesn't coincide with the center of the secondary flow, but it is slightly shifted toward the ridge (Fig. 3). Large negative (positive) vorticity is observed in the up-slope (down-slope) wall along the ridge, that is indicative of the distortion undergone by the streamlines near the inclined walls.

The distortion is such to change the sign of the curvature of the streamlines (and consequently the sign of vorticity) compared to that in the core of the secondary flow (see also Fig. 2).

The distribution of the mean velocity components as well as of the turbulent intensities (both not reported here) showed the LES results to fit very satisfactorily the DNS data.

LES against experiments

In the present section we show the comparison between our LES results and the NN84's data considering the same geometry as in "Case I" of NN84 and the same friction Reynolds number ($Re_\tau = 582$). In "Case I" the ridge spacing is $a = \delta$, the ridge is wide 0.5δ and 0.25δ at the bottom and at the top respectively and it is 0.125δ height.

The streamwise and spanwise extension of the domain has been chosen according to the spatial integral scales reported in the DNS database of Moser *et al.* (1999). Specifically, it has been observed that a $1.25\pi\delta$ long, and 2δ wide domain is enough to simulate the flow accurately. We consider two ridges equispaced over each solid wall, thus considering four ridges put inside the channel.

In the present case the statisticts have been accumulated in time, averaged over the x-direction, over the four ridges and finally over half ridge, thus using all the possible simmetries of the mean flow field .

The number of grid points used is $48\times96\times64$ in the x, y and z directions respectively, that give $\Delta x^+ \sim 48$, $\Delta z^+ \sim 18$ and $1 < \Delta y^+ < 25$.

At $Re_\tau = 582$, the trapezoidal ridge, in wall-units, is 72 height, 291 wide at bottom and 145 wide at the top. After that a turbulent steady state had been reached, the computation has been carried out for $tu_\tau/\delta \sim 15$.

As in the low-Reynolds number case, the presence of a large-scale secondary flow has been detected as well. The LES predicts the center of the vortex located at $y = 0.25\delta$, $z = 0.25\delta$, that is the same as that measured in the experiments. According to NN84, the contour-plot of the mean streamwise velocity (Fig. 4) shows that the obstacle produces mean low-speed zones at the top of the ridge, whereas a high-speed zone is detected over the trough. The vertical distribution of spanwise (w) and vertical (v) velocity components at different spanwise locations are reported in Fig. 5 and in Fig. 6. The maximum spanwise velocity is $w_{max} \sim 0.018U_{max}$ at $z/\delta = 0.296$, $y/\delta = 0.12$, whereas NN84 measured a value

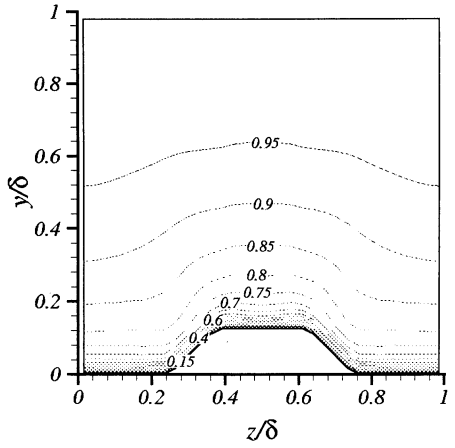

Figure 4: Contour-plot of the mean streamwise velocity (made dimensionless with U_{max}) in the cross-stream section ($Re_\tau = 582$)

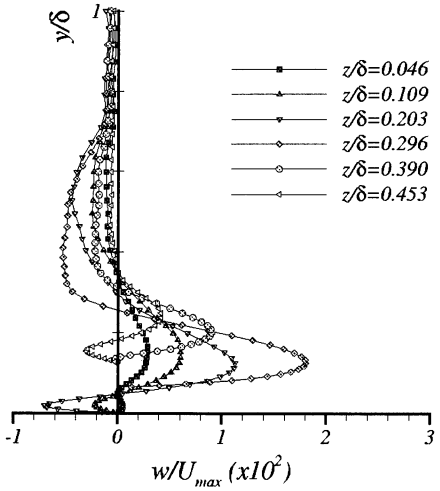

Figure 5: Wall-normal distribution of the spanwise mean velocity component w at several spanwise locations ($Re_\tau = 582$).

$w_{max(NN84)} \sim 0.021U_{max}$ at $z/\delta = 0.250$, $y/\delta = 0.11$; The maximum vertical velocity is $v_{max} \sim 0.02U_{max}$ at $z/\delta = 0.390$, $y/\delta = 0.21$, whereas in NN84 $v_{max(NN84)} \sim 0.015U_{max}$ is measured at $z/\delta = 0.5$, $y/\delta = 0.32$. The above differences indicate that although the center of the secondary flow is the same as in the experiments, a different shape is obtained in our computation. The main cause of such discrepance migth be that the our computational domain doesn't fit completely the experimental setup. Indeed we consider an infinite array of ridges (enforced by periodicity in the spanwise direction) whereas NN84 have considered a small aspect-ratio rectangular duct ($z_{max}/2\delta = 2.25$) with four ridges over each

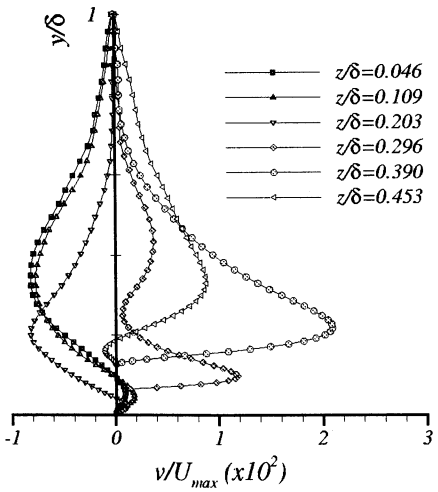

Figure 6: Wall-normal distribution of the vertical mean velocity component v at several spanwise locations (Re_τ = 582).

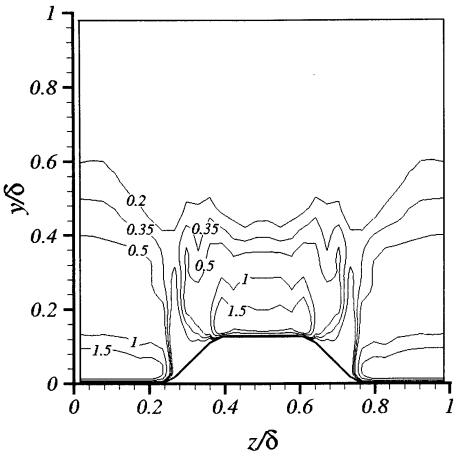

Figure 7: Contour-plot of the difference between the cross-stream resolved normal Reynolds stresses $< w'w' > - < v'v' >$ made dimensionless with U^2_{max} at $Re_\tau = 582$.

wall. In such duct the secondary currents that develop over the ridge interact with those generated by the lateral walls, thus resulting in altered space-distribution of the mean streamwise vorticity.

The vertical distribution of the spanwise velocity component attains a maximum (minimum) near the wall in the trough (top) of the ridge, then it increases (decreases) and finally gets negative (positive); this behaviour is the signature of the secondary flow. A closer look at Fig. 6, shows that in most of the spanwise locations, the vertical velocity changes its sign when approaching the wall, thus indicating the presence of additional small re-circulation zones. This flow pattern has not appeared in the low Reynolds number case. The matter will be highlighted in the next section.

Finally, previous numerical and experimental studies have emphasized the role of the variation of the normal stresses in the cross-stream section ($\frac{\partial^2(<w'w'>-<v'v'>)}{\partial y \partial z}$), since they contribute to the production of the mean streamwise vorticity. In Fig. 7 the contour-plot of $< w'w' > - < v'v' >$ is shown. It can be noticed that the spanwise variation of the differences of the cross-stream normal stresses is negligible either over the ridge and in the trough, whereas it is significant over the inclined walls, indicating that this is the zone where a significant production of streamwise vorticity occurs.

DISCUSSION AND CONCLUDING REMARKS

As above shown, LES results are in good agreement with either the DNS data at Re_τ = 140 and with the experimental ones at a Reynolds number as large as three times the previous one. The remarkable differences between the DNS results and the experimental data can be attributed to the different Reynolds numbers of the flow. Indeed, it has to be noticed that the height of the ridge is different in the two cases *if expressed in wall-units*: in the low Reynolds number case, the ridge is 17.5 wall-units height, thus being completely located within the buffer layer; conversely, in the other case the ridge is 72 wall-units height, hence it is fully exposed in the log-layer. This causes the change of the position and of the intensity of the secondary current. Furthermore,

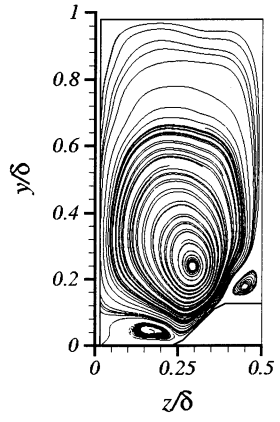

Figure 8: Mean stream-tracers in the cross-stream plane at $Re_\tau = 582$

in the high Reynolds number case only, ad-

ditional near-wall, small, secondary flows appear togheter with the large-scale one which has a diameter $\sim O(\delta)$. These additional re-circulations are promoted by the $(\frac{\partial^2}{\partial z^2} - \frac{\partial^2}{\partial y^2}) < v'w' >$ production term of the mean streamwise vorticity equation. They are respectively located over the ridge and at the bottom corner (Fig. 8). In spite of their small extension, mean vorticity is large there, and comparable with that in the main secondary flow (Fig. 9). The smallness of these near-wall re-circulations togheter with their large intensity may produce large localized secondary shear stresses that may enhance phenomena of local erosion. The presence of the small re-circulations had been argued in previously works. In fact, NN84 noticed the existence of a near-wall zone with vorticity that changes sign along the spanwise direction, that is the signature of a possible re-circulation zone. Further, Colombini (1993)

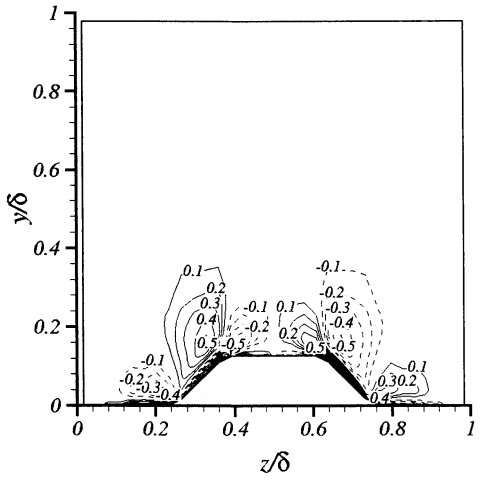

Figure 9: Mean dimensionless streamwise vorticity in the cross-stream plane at $Re_\tau = 582$

has found a similar re-circulation in the trough, but only in a case characterized by a ridge spacing as large as twice that investigated in the present work.

Finally, as in NN84 and in the low-Reynolds number case, the location where the vorticity peaks doesn't coincide with the center of the large secondary flow, rather it appears shifted toward the wall. This has to be associated to the sharp increase of vorticity due to the presence of the wall.

The present research has been jointly supported by S.I.O.T. S.p.A., by the "Prefettura di Trieste" and by the "Istituto Nazionale di Oceanografia e di Geofisica Sperimentale, Trieste".

References

Armenio, V., and Piomelli, U., 2000, "A Lagrangian mixed subgrid-scale model in generalized coordinates", *Flow, Turbulence and Combustion* Vol. 65, pp. 51-81.

Bardina, J., Ferziger, J. H., & Reynolds W.C., 1980, "Improved subgrid scale models for large eddy simulation", *AIAA paper No. 80-1357.*

Colombini, M., 1993, "Turbulence-driven secondary flows and formation of sand ridges", *J. Fluid Mech.*, Vol. 254, pp. 701-719.

Kawamura, H. & Sumori, T., 1999, "DNS of turbulent flow in a channel with longitudinally ridged walls" *Direct and Large-Eddy SimulationIII, Edited by P.R. Voke, N.D. Sandham and L. Kleiser, Kluwer Academic Publ.*, pp. 405-416.

Liu., J., Piomelli, U. & Spalart P. R., 1996, "Interaction between a spatially growing turbulent boundary layer and embedded streamwise vortices" *J. Fluid Mech.*, Vol. 326, pp. 151-179.

Meneveau, C., Lund, T. S. & Cabot, W. H., 1996, "A Lagrangian dynamic subgrid-scale model of turbulence", *J. Fluid Mech.*, Vol. 319, 353-385.

Moser, R. D., Kim, J. & Mansour, N. M., 1999, "Direct numerical simulation of turbulent channel flow up to $Re_\tau = 582$", *Phys. Fluids*, Vol. 11, 943-945.

Muller, A. 1979, "Secondary flow in open channel", *Proc. XVIIIth Congress of the IAHR, No. B.A.3*, pp. 19-24.

Nezu, I & Nakagawa H., 1984, "Cellular secondary currents in straight conduit", *J. of Hydr. Eng.*, Vol. 110, pp. 173-191.

Smagorinsky, J., 1963, "General circulation experiments with the primitive equations: I the basic experiment", *Monthly Weather Review*, Vol. 91, pp. 99-106.

Tominaga, A. & Nezu, I., 1991, "The Effects of secondary currents on sediment transport in open-channel flows", *Proc. Int. Symp. on the Transport of Suspended Sediment and its Mathematical Modelling, Florence, Italy*, pp. 253-264.

Zang., Y., Street, R. L., & Koseff, J., 1994, "A non-staggered grid, fractional step method for the time-dependent incompressible Navier-Stokes equation in curvilinear coordinates", *J. Comp. Phys.*, Vol.114, 18-33.